Overlapping Internal Boundary Control of Lane-free Automated Vehicle Traffic – An LMI Approach *

Milad Malekzadeh, Venkata Karteek Yanumula, Ioannis Papamichail, Markos Papageorgiou, *Life Fellow, IEEE*

***Abstract*— Internal boundary control (IBC) for lane-free automated vehicle traffic has been recently proposed. The total road width and capacity are flexibly shared between the two opposite traffic directions of a highway in real-time to sensibly increase the cross-road infrastructure utilization. Centralized solutions have already been proposed, which, however, may be cumbersome for long highways with respect to the offline controller design effort; the extent of real-time communications; and the physical system architecture. To mitigate these issues, increase system reliability and reduce monitoring and maintenance effort, this paper proposes an overlapping decentralized control scheme for IBC of lane-free automated vehicle traffic by transforming the discrete-time optimal control problem to a linear matrix inequalities (LMI) problem. After selecting the overlapping structure and solving the LMI problem, the correspondingly structured gain matrix may be obtained, enabling a decentralized overlapping control scheme. Simulation investigations demonstrate that the proposed overlapping regulator is similarly efficient as the centralized solutions.**

I. Introduction

Recurrent traffic congestion is a serious problem for most big cities around the globe. Traffic control measures are valuable [1], [2], but not always sufficient to tackle heavily congested traffic conditions. Gradually emerging vehicle automation and communication systems should be exploited to develop innovative solutions that can be applied to smart road infrastructures [3].

A novel traffic paradigm, called TrafficFluid, applicable to high penetration rates of vehicles equipped with high levels of vehicle automation and communication systems has been proposed recently [4]. Lane-free traffic is one of the features of the TrafficFluid concept, according to which vehicles can move without being bound to fixed traffic lanes. In this context, it becomes possible to employ internal boundary control (IBC), a promising and innovative control measure aiming to achieve an unprecedented exploitation of the available road infrastructure [5]. IBC relies on the fact that, in lane-free traffic, the traffic flow and capacity may exhibit incremental changes in response to corresponding incremental changes of the road width. Thus, on a highway or arterial with two opposite traffic directions, the total cross-road capacity (for both directions) may be shared between the two directions in real-time, according to the prevailing demand per direction, by virtually moving the internal boundary that separates the two traffic directions and communicating this decision to CAVs (Connected Automated Vehicles), so that they respect the changed road boundary. This calls for an appropriate real-time control strategy that changes to internal road boundary in space and time, as illustrated in Fig. 1, in response to the current traffic conditions, to maximize the traffic efficiency in both directions.

The characteristics of the IBC problem are analyzed in [5], [6], and solutions have been provided based on an optimal open-loop control approach, in the form of a convex Quadratic Programming (QP) problem [5], as well as via feedback-based Linear-Quadratic Regulators (LQR), aiming at balancing the relative densities in the two directions [6]. However, for very long highways, the unique (centralized) LQR applying to the whole highway may have to be designed with hundreds of state variables; also, its application requires real-time information from the whole highway under consideration, which may be problematic for very long highways with respect to the required communications and physical system architecture.

Various concepts for large-scale and geographically extended systems were proposed in the last decades to address control challenges that cannot be unraveled via centralized control methods. Such systems typically comprise various local control stations, each in charge of the operation of a part of the overall system. The overall control system objective is achieved or approximated via local control system actions, i.e., via a decentralized control system. The control engineer may define the configuration of subsystems, and local controllers are constructed with the purpose of the overall system stability and performance being satisfied [7] under the motto “think global, act local”. The disjoint decomposition of the global system is not reasonable if the subsystems are strongly interconnected. To address this

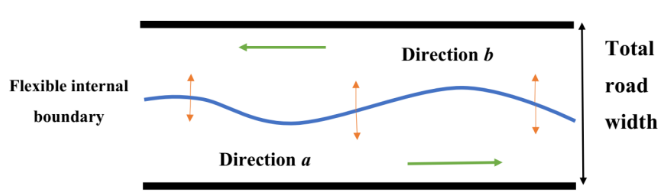

Figure 1. Space-time flexible internal road boundary.

* The research leading to these results has received funding from the European Research Council under the European Union’s Horizon 2020 Programme / ERC Grant Agreement no. 833915, project TrafficFluid, see: https://www.trafficfluid.tuc.gr.

All authors are with the Dynamic Systems and Simulation Laboratory, Technical University of Crete, Chania, Crete, 73100, Greece. Markos Papageorgiou is also with the Faculty of Maritime and Transportation, Ningbo University, Ningbo, China. (e-mails: mmalek@dssl.tuc.gr; karteek@dssl.tuc.gr; ipapa@dssl.tuc.gr; markos@dssl.tuc.gr).

problem, an overlapping control scheme can be a remedy, whereby the overlapping area creates a connection between two neighboring subsystems, so as to enhance the performance of the decentralized control [8].

Several overlapping control strategies have been proposed in the literature. This paper introduces an overlapping decentralized control scheme for IBC of lane-free automated vehicle traffic using linear matrix inequalities (LMI). The discrete-time LQR problem is first transformed into a linear matrix inequalities (LMI) problem [9]. After selecting the overlapping structure and solving the LMI problem, the correspondingly structured gain matrix is obtained, enabling a decentralized overlapping control scheme. Simulation investigations, involving a realistic highway stretch and demand scenario, demonstrate that the proposed regulator is similarly efficient as the central LQR and the open-loop QP solution.

Section II presents some background issues, while Section III presents the design of the overlapping regulator. Simulation investigations are presented in Section IV, while conclusions are given in Section V.

II. Background

Some background, necessary for understanding modelling and controller design for IBC, is provided in this section for completeness.

A. *Modelling for Internal Boundary Control*

Lane-free traffic is not expected to give rise to structural changes of existing macroscopic traffic flow models, and notions like the conservation equation, the Fundamental Diagram (FD), as well as moving traffic waves will continue to characterize macroscopic traffic flow modelling. An extended version of CTM (Cell Transmission Model), a first-order dynamic traffic flow model with a triangular FD [10], is considered in what follows.

We call the two opposite traffic directions, presented in Fig. 1, directions a (from left to right) and b (from right to left). The considered freeway stretch is subdivided into n sections, with respective lengths L_i, $i = 1, 2, \dots, n.$ The total road width (both directions) $w,$ which is assumed constant over all sections for simplicity, can be flexibly shared between the two directions of each section in real-time. Specifically, each direction is assigned a corresponding road width $w_i^a = \varepsilon_i \cdot w$ and $w_i^b = (1-\varepsilon_i) \cdot w,$ where $0 \le \varepsilon_i \le 1$ is the sharing factor per section $i = 1, 2, \dots, n,$ to be specified in real-time as a control input by the internal boundary controller. The total section capacity q_{cap}, as well as the critical density ρ_{cr} and the jam density $\rho_{\max}$, are shared between the two traffic directions a and $b.$ Based on the derivation presented in [5], the sharing equations are given by

$$q_{i,cap}^a(\varepsilon_i) = \varepsilon_i \cdot q_{cap},\; q_{i,cap}^b(\varepsilon_i) = (1-\varepsilon_i)\cdot q_{cap}$$
$$\rho_{i,cr}^a(\varepsilon_i) = \varepsilon_i \cdot \rho_{cr},\; \rho_{i,cr}^b(\varepsilon_i) = (1-\varepsilon_i)\cdot \rho_{cr} \qquad (1)$$
$$\rho_{i,\max}^a(\varepsilon_i) = \varepsilon_i \cdot \rho_{\max},\; \rho_{i,\max}^b(\varepsilon_i) = (1-\varepsilon_i)\cdot \rho_{\max}$$

where, for simplicity, the assumption was made that sharing of traffic quantities in the two directions is symmetric, something that is not exact for freeways where capacity per meter-width in direction a is different than for direction b, i.e., the total capacity q_{capi} of each section (both directions) is not constant, but a function of the sharing factor ε_i.

To disallow the complete closure of either direction, the assigned road width in either direction should never be less than the widest vehicles driving on the road. This requirement gives rise to stricter constraints

$$0 < \varepsilon_{i,\min} \le \varepsilon_i \le \varepsilon_{i,\max} < 1 \qquad (2)$$

where $\varepsilon_{i,\min} \cdot w$ and $(1-\varepsilon_{i,\max}) \cdot w$ are the minimum admissible widths for directions a and $b,$ respectively.

Another restriction to be applied to the sharing factors concerns the time-delay needed to evacuate traffic on the direction that receives a restricted width, compared to the previous control time-step. Clearly, the time-delay should apply only to the traffic direction that is being widened, compared to the previous control interval; while the direction that is restricted should promptly apply the smaller width, so that CAVs therein move out of the reduced-width zone. Assume that the required time-delay is smaller than or equal to the control time interval T_c; then, the time-delay requirement is automatically fulfilled if the sharing factors that are actually applied to the two directions, i.e. ε_i^a and ε_i^b, respectively, are calculated as follows

$$\varepsilon_i^a(k_c) = \min\{\varepsilon_i(k_c), \varepsilon_i(k_c-1)\}$$
$$\varepsilon_i^b(k_c) = \min\{1-\varepsilon_i(k_c), 1-\varepsilon_i(k_c-1)\} \qquad (3)$$

where $k_c = 0, 1, \dots$ is the discrete control time index. It is noted that the notation $\varepsilon_i^a(k_c)$ and $\varepsilon_i^b(k_c)$ indicates that the sharing factors are applied for the duration of the control time interval $[k_c \cdot T_c, (k_c+1)\cdot T_c)$.

Traffic flows from section 1 to section n in direction a; and from section n to section 1 in direction b (see Fig. 2). We denote ρ_i^a, $i = 1, 2, \dots, n,$ the traffic density of section $i,$ direction a; and ρ_i^b, $i = 1, 2, \dots, n,$ the traffic density of section $i,$ direction $b.$ Similarly, we denote q_i^a and q_i^b, $i = 1, 2, \dots, n,$ the mainstream exit flows of section i for directions a and $b,$ respectively. Thus, q_0^a is the feeding upstream mainstream inflow for direction a; and q_{n+1}^b is the feeding upstream mainstream inflow for direction $b.$ Every section may have an on-ramp or an off-ramp at its upstream boundary. The on-ramp flows (if any) at section i are denoted r_i^a for direction $a,$ and r_i^b for direction $b.$ The off-ramp flow (if any) of section $i,$ direction $a,$ is calculated based on known exit rates β_i^a multiplied with the upstream-section flow, i.e. $\beta_i^a q_{i-1}^a$; and the off-ramp flow (if any) of section $i,$ direction $b,$ is calculated based on known exit rates β_i^b multiplied with the upstream-section flow, i.e. $\beta_i^b q_{i+1}^b.$ The conservation equation for the section i of direction a reads:

$$\rho_i^a(k+1) = \rho_i^a(k) + \frac{T}{L_i}((1-\beta_i^a)q_{i-1}^a(k) - q_i^a(k) + r_i^a(k)) \quad (4)$$

where T is the model time-step, typically set equal to 5–10 s for section lengths of some 500 m, and $k = 0,1,\ldots$ is the corresponding discrete-time index of the model.

According to CTM, traffic flow is obtained as the minimum of demand and supply functions, except for the last section, where only the demand function is considered, assuming that the downstream traffic conditions are uncongested. Considering the impact of the respective sharing factors on the FDs, we have

$$q_i^a(k) = \min\left\{Q_D(\rho_i^a(k), \varepsilon_i(k)), \frac{Q_S(\rho_{i+1}^a(k), \varepsilon_{i+1}(k))}{(1-\beta_{i+1}^a)} - r_{i+1}^a(k)\right\},$$
$$i = 1,2,\ldots,n-1$$
$$q_n^a(k) = Q_D(\rho_n^a(k), \varepsilon_n(k)) \quad (5)$$

The demand and supply functions are given by the following respective equations

$$Q_D(\rho,\varepsilon) = \min\left\{\varepsilon q_{cap}, v_f \rho\right\}$$
$$Q_S(\rho,\varepsilon) = \min\left\{\varepsilon q_{cap}, w_s(\varepsilon\rho_{\max} - \rho)\right\} \quad (6)$$

where v_f is the free speed (which is assumed equal for all sections for simplicity) and w_s is the back-wave speed. The equations for section i of direction b are analogous to those of direction a, with few necessary index modifications, and are therefore omitted here, see [5] for details.

In conventional traffic management, traffic densities reflect explicitly the state of the traffic. However, in IBC, the critical density for each direction and section is a function of the sharing factor and is changing based on the applied control action. The following relations define the *relative density* (dimensionless) of section i and direction a or b

$$\tilde{\rho}_i^a(k) = \frac{\rho_i^a(k)}{\varepsilon_i(k-1)\rho_{cr}}, \; \tilde{\rho}_i^b(k) = \frac{\rho_i^b(k)}{(1-\varepsilon_i(k-1))\rho_{cr}} \quad (7)$$

If the relative density of a section and direction is less than 1, it reflects under-critical traffic conditions; if it is equal to 1, it reflects capacity flow; and if it is greater than 1, it reflects over-critical conditions.

To obtain a state-space model form, the one-step retarded control input is defined as a new state variable according to $\gamma_i(k+1) = \varepsilon_i(k), \quad i = 1,2,\ldots,n.$ Linearization of the overall system of dynamic equations around a nominal point was presented in [6], leading to the linear state-space model

$$\mathbf{x}(k+1) = \mathbf{A}\mathbf{x}(k) + \mathbf{B}\mathbf{u}(k) \quad (8)$$

where $\mathbf{x}(k) = [\Delta\tilde{\rho}_1^a(k), \Delta\tilde{\rho}_1^b(k), \Delta\gamma_1(k), ..., \Delta\tilde{\rho}_n^a(k), \Delta\tilde{\rho}_n^b(k), \Delta\gamma_n(k)]^T$ is the state vector and $\mathbf{u}(k) = \boldsymbol{\Delta\varepsilon}(k)$ is the control vector, whereby $\boldsymbol{\Delta\varepsilon}(k) = [\Delta\varepsilon_1(k), \ldots, \Delta\varepsilon_n(k)]^T$. Also, $\Delta(.)(k) = (.)(k) - (.)^N$, where the superscript N denotes the nominal point, and it has been assumed that $\Delta(.)(k) = 0$ for all disturbances (upstream mainstream inflow, as well as the on-ramp flows of each direction). $\mathbf{A} \in \mathbb{R}^{3n\times 3n}$ and $\mathbf{B} \in \mathbb{R}^{3n\times n}$ are the state and input matrices, respectively.

If the control time-step is a multiple of the model time-step, i.e. $T_c = MT$, where M is an integer, then the discrete control time index is $k_c = \lfloor kT/T_c \rfloor$. Thus, the linear state-space equation may be changed as follows, in order to be based on the control time-step T_c,

$$\mathbf{x}(k_c+1) = \hat{\mathbf{A}}\mathbf{x}(k_c) + \hat{\mathbf{B}}\mathbf{u}(k_c) \quad (9)$$

where $\hat{\mathbf{A}} = \mathbf{A}^M$, and $\hat{\mathbf{B}} = (\mathbf{A}^{M-1} + \mathbf{A}^{M-2} + ... + \mathbf{I})\mathbf{B}$.

B. Centralized LQR design for Internal Boundary Control

When employing the LQR methodology [6], the control goal is the minimization of the quadratic criterion

$$J = \frac{1}{2}\sum_{k_c=0}^{\infty}\left[\mathbf{x}^T(k_c)\mathbf{Q}\mathbf{x}(k_c) + \mathbf{u}^T(k_c)\mathbf{R}\mathbf{u}(k_c)\right] \quad (10)$$

where $\mathbf{Q} \in \mathbb{R}^{3n\times 3n}$ is a symmetric positive semidefinite matrix and $\mathbf{R} \in \mathbb{R}^{n\times n}$ is a symmetric positive definite matrix, subject to the linear state-space equation (9). The nominal value of relative densities on both directions is set equal to 1, so that the controller is motivated to operate the system near capacity. In particular, due to the quadratic penalty terms, the controller tends to mitigate strong density departures from the critical density at specific sections, i.e., mitigate traffic congestion. In addition, if capacity flow is not feasible (e.g. due to lack of demand), then minimizing a sum of squares has the tendency to balance deviations from the nominal values at different sections and directions, something that is conform with the secondary operational sub-objective of balancing the margin to capacity across sections and directions. On the other hand, we set to 0.5 the nominal value for the sharing factors, so as to have smooth and moderate internal boundary changes. Thus, minimization of the second term in (10) mitigates deviations of the sharing factors from 0.5 and balances these deviations in space and time, as unnecessarily strong internal boundary changes over space and time should be avoided.

The optimal controller minimizing the criterion (10) subject to the model (9) is given by a linear state-feedback control law of the form $\mathbf{u}(k_c) = \bar{\mathbf{K}}\mathbf{x}(k_c)$, where $\bar{\mathbf{K}} \in \mathbb{R}^{n\times 3n}$ is a constant gain matrix given by

$$\bar{\mathbf{K}} = (\mathbf{R} + \mathbf{B}^T\mathbf{P}\mathbf{B})^{-1}\mathbf{B}^T\mathbf{P}\mathbf{A} \quad (11)$$

and $\mathbf{P}$ is a unique positive semidefinite solution of the discrete-time algebraic Riccati equation.

III. Overlapping Control Scheme using LMI

Summarizing from above, each highway section has three state variables and one control input, which is the corresponding sharing factor. For very long highways, designing the centralized LQR calls for the solution of an accordingly large-scale Riccati equation. More importantly, the centralized LQR requires real-time information for all the states of the system, even very remote ones, to compute each control input. This requirement may be problematic for long highways due to the need to transfer data from the whole highway in order to compute each sharing factor. Also, the traffic situation may be quite different at different parts of a long highway; then, balancing relative densities and sharing factors over the whole highway may not be fully relevant, as we are interested in addressing this sub-objective primarily at local levels.

For the above reasons, there is an interest in developing a decentralized control scheme, which may reduce the LQR design complexity; reduce the burden of real-time data transferring; reduce the effort of control system monitoring and maintenance and increase the system reliability in cases of device failure. Due to strong dependencies between consecutive sections in traffic flow, developing a fully decentralized control scheme (with disjoint subsystems) may reduce the control efficiency compared to the centralized case, as was indeed confirmed in preliminary investigations. Therefore, in this study, an overlapping control scheme is adopted and tested for IBC. The approach relies on the separation of the highway in a number of subsequent subsystems (highway stretches) which are overlapping, i.e., adjacent subsystems have some sections in common; hence, adjacent subsystems share some states and some control inputs. This approach delivers overlapping decentralized controllers, where, thanks to the overlapping structure, subsystems remain partly aware about the inter-relations with adjacent subsystems.

The quadratic criterion (10) can be rewritten as follows

$$J = \frac{1}{2}\sum_{k_c=0}^{\infty}\left[(\mathbf{Q}^{1/2}\mathbf{x}(k_c))^T\mathbf{Q}^{1/2}\mathbf{x}(k_c) + (\mathbf{R}^{1/2}\mathbf{u}(k_c))^T\mathbf{R}^{1/2}\mathbf{u}(k_c)\right] \tag{12}$$

Let

$$\mathbf{C} = \begin{bmatrix} \left(\frac{1}{2}\mathbf{Q}\right)^{1/2} \\ 0_{n\times 3n} \end{bmatrix}, \quad \mathbf{D} = \begin{bmatrix} 0_{3n\times n} \\ \left(\frac{1}{2}\mathbf{R}\right)^{1/2} \end{bmatrix} \tag{13}$$

and $\mathbf{Z}(k_c) = \mathbf{C}\mathbf{x}(k_c) + \mathbf{D}\mathbf{u}(k_c)$. Using the above, the objective function (12) becomes

$$J = \sum_{k=0}^{\infty}\mathbf{Z}^T(k_c)\mathbf{Z}(k_c) \tag{14}$$

If we assume the use of a linear feedback control law

$$\mathbf{u}(k_c) = \mathbf{K}\mathbf{x}(k_c) \tag{15}$$

then we have $\mathbf{Z}(k_c) = (\mathbf{C}+\mathbf{D}\mathbf{K})\mathbf{x}(k_c)$ and (14) becomes

$$J = \sum_{k=0}^{\infty}\left[\mathbf{x}^T(k_c)(\mathbf{C}+\mathbf{D}\mathbf{K})^T(\mathbf{C}+\mathbf{D}\mathbf{K})\mathbf{x}(k_c)\right]. \tag{16}$$

Using the trace operator $\mathbf{Tr}(.)$, (16) becomes

$$J = \sum_{k=0}^{\infty}\mathbf{Tr}\left((\mathbf{C}+\mathbf{D}\mathbf{K})\mathbf{x}(k_c)\mathbf{x}^T(k_c)(\mathbf{C}+\mathbf{D}\mathbf{K})^T\right) = \mathbf{Tr}\left((\mathbf{C}+\mathbf{D}\mathbf{K})\mathbf{P}(\mathbf{C}+\mathbf{D}\mathbf{K})^T\right) \tag{17}$$

where $\mathbf{P} = \sum_{k=0}^{\infty}\mathbf{x}(k_c)\mathbf{x}^T(k_c)$ is a symmetric positive definite matrix satisfying the following Lyapunov equation [11] for the linear state-space model (9) after using the feedback law (15)

$$\mathbf{P} - (\hat{\mathbf{A}}+\hat{\mathbf{B}}\mathbf{K})\mathbf{P}(\hat{\mathbf{A}}+\hat{\mathbf{B}}\mathbf{K})^T - \mathbf{x}_0\mathbf{x}_0^T = 0 \tag{18}$$

with $\mathbf{x}_0 = \mathbf{x}(0)$. Then, if we define $\gamma \in (0,1)$, the following holds

$$\mathbf{P} - (\hat{\mathbf{A}}+\hat{\mathbf{B}}\mathbf{K})\mathbf{P}(\hat{\mathbf{A}}+\hat{\mathbf{B}}\mathbf{K})^T - \gamma^2\mathbf{x}_0\mathbf{x}_0^T > 0 \tag{19}$$

Considering a matrix $\mathbf{F} \in \mathbb{R}^{n\times 3n}$ given by $\mathbf{F} = \mathbf{K}\mathbf{P}$, the objective function becomes

$$J = \mathbf{Tr}\left((\mathbf{C}+\mathbf{D}\mathbf{F}\mathbf{P}^{-1})\mathbf{P}(\mathbf{C}+\mathbf{D}\mathbf{F}\mathbf{P}^{-1})^T\right) = \mathbf{Tr}\left((\mathbf{C}\mathbf{P}+\mathbf{D}\mathbf{F})\mathbf{P}^{-1}(\mathbf{C}\mathbf{P}+\mathbf{D}\mathbf{F})^T\right) \tag{20}$$

and (19) becomes,

$$\mathbf{P} - (\hat{\mathbf{A}}\mathbf{P}+\hat{\mathbf{B}}\mathbf{F})\mathbf{P}^{-1}(\hat{\mathbf{A}}\mathbf{P}+\hat{\mathbf{B}}\mathbf{F})^T - \gamma^2\mathbf{x}_0\mathbf{x}_0^T > 0 \tag{21}$$

Using the Schur complement lemma [12] for an auxiliary variable $\mathbf{W} > (\mathbf{C}\mathbf{P}+\mathbf{D}\mathbf{F})\mathbf{P}^{-1}(\mathbf{C}\mathbf{P}+\mathbf{D}\mathbf{F})^T$ and for (21), we can formulate the following optimization problem

$$\begin{gathered} \min \mathbf{Tr}(\mathbf{W}) \\ \begin{bmatrix} \mathbf{W} & \mathbf{C}\mathbf{P}+\mathbf{D}\mathbf{F} \\ * & \mathbf{P} \end{bmatrix} > 0 \\ \begin{bmatrix} \mathbf{P} & \hat{\mathbf{A}}\mathbf{P}+\hat{\mathbf{B}}\mathbf{F} & \gamma\mathbf{x}_0 \\ * & \mathbf{P} & 0 \\ * & * & \mathbf{I} \end{bmatrix} > 0 \end{gathered} \tag{22}$$

The discrete-time LQR problem has now been transformed to a linear matrix inequalities (LMI) problem that can be solved using infeasible path-following algorithms for solving standard semidefinite programs [13] in order to get the optimal matrices $\mathbf{F}$ and $\mathbf{P}$. The difference compared to the discrete-time LQR problem is that we can now specify the structure of the resulting gain matrix $\mathbf{K}$ before solving the LMI problem by specifying the structure of the matrices $\mathbf{F}$ and $\mathbf{P}$. This way, we can design an overlapping decentralized control scheme for IBC of lane-free automated vehicle traffic.

IV. Simulation Investigation

A. Simulation set-up

The performance of the proposed overlapping control scheme is investigated using the bi-directional highway stretch depicted in Fig. 2. The considered highway stretch has a length of 5 km and is subdivided into 10 sections of 0.5 km each. The modelling time-step, T, is set to 10 s, and the considered time horizon is 1 h. While a linearization of CTM was used for controller design, the full nonlinear CTM is used to represent the emulated ground truth in this section. The model parameters used are $v_f = 100$ km/h and $w_s = 12$ km/h; while the total cross-road capacity to be

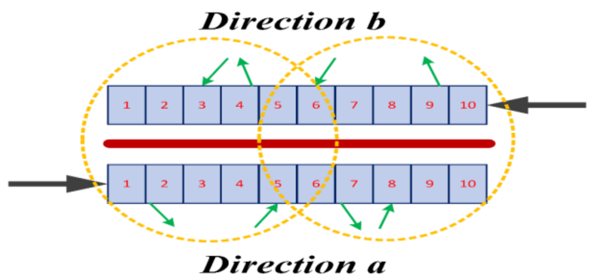

Figure 2. The considered highway stretch.

shared among the two directions is $q_{cap} = 12{,}000$ veh/h. The exit rates for the four off-ramps are all set equal to 0.1.

The mainstream and on-ramp demand flows per direction are presented in Fig. 3. It may be seen that the two directions feature respective peaks in their mainstream demands that are slightly overlapping. The on-ramp demands are constant and are all equal to 1000 veh/h. The simulation results of the no-control case are presented first, followed by the results obtained when using the decentralized LMI-based control scheme.

B. No-control case

When no internal boundary control is applied, the total width of the highway stretch is equally shared to the two directions, i.e., the sharing factor ε_i is constant and equal to 0.5 for all sections. Using the demand profiles presented in Fig. 3 in the nonlinear CTM model with $\varepsilon_i = 0.5$, we get the simulation results for the no-control case. Figure 4 displays the corresponding spatio-temporal evolution of the relative density defined in (7). According to the definition, relative density values lower than 1 refer to uncongested traffic; while values higher than 1 refer to congested traffic; when the relative density equals 1, and the downstream section is uncongested, we have capacity flow at the corresponding section.

Figure 4 shows that congestion is created in sections 5 and 8 for direction a due to the increased mainstream demand, in combination with the ramp inflows, at around $k = 70$. The congestion dissolves at around $k = 160$, due to the rapid decrease of the mainstream demand for this direction. In direction b, we have also congestion being triggered in sections 3 and 6 for similar reasons, at around $k = 240$. The congestion dissolves at around $k = 340$. The Total Time Spent by all vehicles in the highway stretch (TTS) is equal to 314.6 veh·h.

C. Control case

In order to apply the feedback regulator (15), we need to calculate off-line the static gain matrix $\mathbf{K}$. For this, we need first to solve the optimization problem (22) and obtain matrices $\mathbf{F}$ and $\mathbf{P}$. A nominal point of operation is selected for the calculation of the matrices $\hat{\mathbf{A}}$ and $\hat{\mathbf{B}}$ used in the linear model (9) and also required in (22). The nominal values are $q_0^a\big|_N = q_{11}^b\big|_N = 5000$ veh/h, $r_5^a\big|_N = r_8^a\big|_N = r_3^b\big|_N = r_6^b\big|_N = 1000$ veh/h, $\tilde{\rho}_i^a\big|_N = \tilde{\rho}_i^b\big|_N = 1$ and $\varepsilon_i\big|_N = 0.5$, $i = 1, 2, \ldots, 10$. The control time-step, T_c, is set to 60 s, hence $M = 6$. The weighing matrices used in the objective function (12), and required for the definition of matrices $\mathbf{C}$ and $\mathbf{D}$ in (13), are selected to be $\mathbf{Q} = \mathbf{I}_{3n\times 3n}$ and $\mathbf{R} = 10^{-3}\mathbf{I}_{n\times n}$. These values were specified in a trial-and-error procedure and were found to work properly for other traffic scenarios as well.

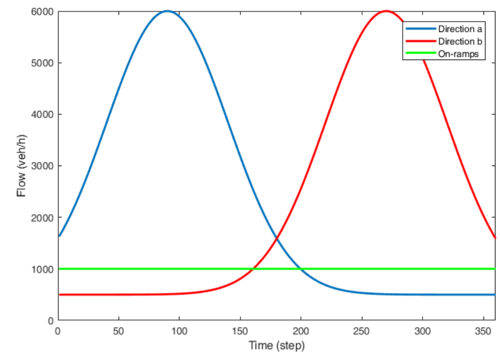

Figure 3. Demand flows per direction and on-ramp.

The overlapping control structure is selected to be conform with the one-dimensional interacting structure of traffic flow. In both directions, each relative density state of the linearized model depends on the state of the upstream section. As a result, if, for the case of the considered highway, we select to work with two subsystems, these subsystems will have to share an overlapping area of two sections. As can be seen in Fig. 2, we are considering two subsystems with six segments each; thus segments 5 and 6 are taken into account as an overlapping area. The application of such an overlapping control structure requires the following structure for the gain matrix

$$\mathbf{K}_{10\times 30} = \begin{bmatrix} \mathbf{K}^1_{4\times 18} & \mathbf{0} \\ \hdashline & \mathbf{K}^{1,2}_{2\times 30} \\ \hdashline \mathbf{0} & \mathbf{K}^2_{4\times 18} \end{bmatrix} \tag{23}$$

In order to obtain the above, the following structure can be considered for matrices $\mathbf{F}$ and $\mathbf{P}$.

$$\mathbf{F}_{10\times 30} = \begin{bmatrix} \mathbf{F}^1_{4\times 18} & \mathbf{0} \\ \hdashline & \mathbf{F}^{1,2}_{2\times 30} \\ \hdashline \mathbf{0} & \mathbf{F}^2_{4\times 18} \end{bmatrix}, \ \mathbf{P} = \begin{bmatrix} P_1 & 0 & \dots & \dots & 0 \\ 0 & P_2 & 0 & \dots & 0 \\ 0 & \ddots & \ddots & \ddots & \vdots \\ \vdots & \ddots & \ddots & \ddots & 0 \\ 0 & \cdots & 0 & 0 & P_{30} \end{bmatrix} \tag{24}$$

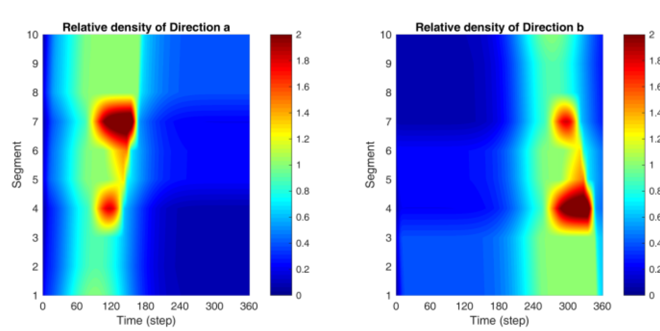

Figure 4. Relative density for the two directions in the no-control case.

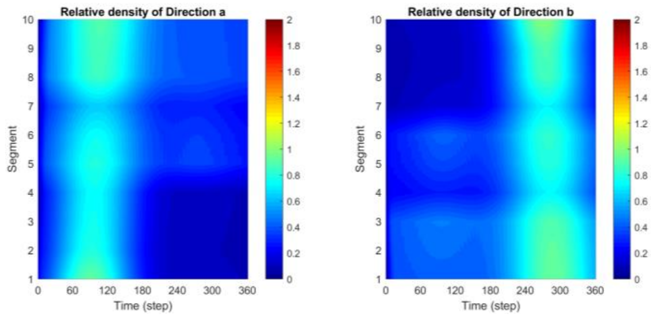

Figure 5. Relative density for the two directions in the control case.

The feedback regulator (15) is used with $\gamma_i(0)$ set equal to the nominal values, i.e. equal to 0.5 for all sections $i = 1, 2, \ldots, 10$. The regulator is operated in a closed-loop mode, receiving in emulated real time all section density values per direction from the CTM model equations; and responding with the sharing factors computed according to (15). The upper and lower bounds for the sharing factors, used to avoid blocking of any of the two directions, are equal for all sections $i = 1, 2, \ldots, 10$ and are given the values $\varepsilon_{i,\min} = 0.16$ and $\varepsilon_{i,\max} = 0.84$. This control loop is repeated every $T_c = 60\,\mathrm{s}$.

The resulting traffic conditions are under-critical everywhere as shown in the spatio-temporal evolution of the relative densities depicted in Fig. 5. The achieved TTS value is 288.9 veh·h, indicating an improvement of 8.2% over the no-control case. The TTS value obtained using the overlapping decentralized control scheme is, in fact, equal to the value that is achieved when applying the optimal control resulting from the QP problem formulation or the LQR formulation presented by the authors in [5] and [6], respectively. Thus, despite the use of a decentralized control scheme, where no demand predictions are necessary and the need for communication is reduced, the proposed approach achieves the highest possible efficiency for the investigated scenario.

V. Conclusion

The concept of internal boundary control (IBC), introduced in [5], has been revisited in this study by use of a different control approach. The well-known CTM, appropriately adjusted to introduce the effect of the sharing factors, has been utilized for the development of an overlapping decentralized regulator for the IBC problem. An LMI approach has been utilized to this end. The total road width and capacity are shared in each section in real-time among the two directions of the road in response to the prevailing traffic conditions. The regulator is easy to design and implement (feedback-based) and robust to disturbances (no need to predict the arriving demands). Simulation investigations demonstrate that the overlapping decentralized control scheme is as efficient as an open-loop optimal control solution (with perfect model knowledge and demand prediction) developed for the same problem in [5] using a convex QP problem formulation or the LQR formulation presented by the authors in [6].

Ongoing work considers microscopic simulation studies with vehicles moving in a lane-free mode, based on appropriate CAV movement strategies developed in the frame of the Trafficfluid project [4], [14],[15].

References

[1] M. Papageorgiou, C. Diakaki, V. Dinopoulou, A. Kotsialos, and Y. Wang, “Review of road traffic control strategies,” *Proceedings of the IEEE*, vol. 91, no. 12, pp. 2043–2067, 2003.

[2] A.A. Kurzhanskiy, and P. Varaiya, “Active traffic management on road networks: a macroscopic approach,” *Philosophical Transactions of the Royal Society A: Mathematical, Physical and Engineering Sciences*, vol. 368, no. 1928, pp. 4607–4626, 2010.

[3] C. Diakaki, M. Papageorgiou, I. Papamichail, and I. Nikolos, “Overview and analysis of vehicle automation and communication systems from a motorway traffic management perspective,” *Transportation Research Part A*, vol. 75, pp. 147–165, 2015.

[4] M. Papageorgiou, K.S. Mountakis, I. Karafyllis, I. Papamichail, and Y. Wang, “Lane-free artificial-fluid concept for vehicular traffic,” *Proceeding of the IEEE*, vol. 109, pp. 114–121, 2021.

[5] M. Malekzadeh, I. Papamichail, M. Papageorgiou, and K. Bogenberger, “Optimal internal boundary control of lane-free automated vehicle traffic,” *Transportation Research Part C*, vol. 126, Article 103060, 2021.

[6] M. Malekzadeh, I. Papamichail, and M. Papageorgiou, “Linear-Quadratic regulators for internal boundary control of lane-free automated vehicle traffic,” *Control Engineering Practice*, vol. 115, 104912, 2021.

[7] L. Bakule, “Decentralized control: Status and outlook,” *Annual Reviews in Control*, vol. 38, no. 1, pp.71–80, 2014.

[8] L. Bakule, J. Rodellar, and J.M. Rossell, “Robust overlapping guaranteed cost control of uncertain state-delay discrete-time system,” *IEEE Transactions on Automatic Control*, vol. 51, no. 12, pp.1943–1950, 2006.

[9] A.I. Zečević and D.D. Šiljak, “A new approach to control design with overlapping information structure constraints,” *Automatica*, vol. 41, no. 2, pp. 265–272, 2005.

[10] C. F. Daganzo, “The cell transmission model: A dynamic representation of highway traffic consistent with the hydrodynamic theory,” *Transportation Research Part B: Methodological*, vol. 28, no. 4, pp. 269–287, 1994.

[11] B.N. Datta, *Numerical methods for linear control systems*. Elsevier Academic Press, 2004.

[12] J.G. Van Antwerp, and R.D. Braatz, “A tutorial on linear and bilinear matrix inequalities,” *Journal of Process Control*, vol. 10, no. 4, pp. 363–385, 2000.

[13] K.C. Toh, M. J. Todd, and R. H. Tütüncü, “SDPT3 - A Matlab software package for semidefinite programming Version 1.3,” *Optimization Methods and Software*, vol. 11, pp. 545–581, 1999.

[14] M. Malekzadeh, D. Manolis, I. Papamichail, and M. Papageorgiou, “Empirical investigation of properties of lane-free automated vehicle traffic,” *25th IEEE International Conference on Intelligent Transportation Systems (ITSC 2022)*, Macau, China, October 8-12, 2022, pp. 2393–2400.

[15] V.K. Yanumula, P. Typaldos, D. Troullinos, M. Malekzadeh, I. Papamichail, M. Papageorgiou, “Optimal path planning for connected and automated vehicles in lane-free traffic with vehicle nudging,” http://arxiv.org/abs/2207.09670.